Pergamon

Polyhedron Vol. 14, No. 19, pp. 2771–2785, 1995
Elsevier Science Ltd
Printed in Great Britain
0277–5387/95 $9.50+0.00

0277–5387(95)00144–1

AN INVESTIGATION OF THE FLUXIONALITY OF $[Fe_3(CO)_{11}(CNBu^t)]$ AND $[Fe_3(CO)_{10}(CNBu^t)\{P(OMe)_3\}]$, AND THE X-RAY STRUCTURE OF $[Fe_3(CO)_{10}(CNBu^t)\{P(OMe)_3\}]$*

HARRY ADAMS, ANDREW G. CARR, BRIAN E. MANN† and ROBERT MELLING

Department of Chemistry, The University of Sheffield, Sheffield S3 7HF, U.K.

Abstract—$[Fe_3(CO)_{11}(CNBu^t)]$ and $[Fe_3(CO)_{10}(CNBu^t)\{P(OMe)_3\}]$ have been examined by variable temperature ^{13}C and, in the latter case, ^{31}P NMR spectroscopy. At low temperatures both compounds are undergoing a rapid concerted bridge-opening bridge-closing carbonyl exchange. This results in a carbonyl ^{13}C NMR spectrum for $[Fe_3(CO)_{11}(CNBu^t)]$ which consists of three signals in the ratio 1:5:5. $[Fe_3(CO)_{10}(CNBu^t)\{P(OMe)_3\}]$ shows two sets of ^{13}CO signals at low temperature, each in the ratio 1:2:2:2:2:1. The two major isomers present have been identified. The X-ray structure of one of the isomers of $[Fe_3(CO)_{10}(CNBu^t)\{P(OMe)_3\}]$ has been determined.

The nature of $[Fe_3(CO)_{12}]$ has been a challenge since its discovery in 1906.[1] For many years the structure was in doubt,[2] but with the use of X-ray crystallography the structure was proven.[2,3] Even the X-ray structure determinations have left question marks about the detailed solid-state structure, as it was found that the asymmetry of the bridging carbonyls is temperature dependent.[3b,c]

The solution structure of $[Fe_3(CO)_{12}]$ is still to be established. IR spectroscopic investigations have left the solution structure of $[Fe_3(CO)_{12}]$ in question. The spectrum consists of two strong, well defined bands in the terminal stretching region and two weak bands in the bridging carbonyl region.[4] The nature of these weak bands in the bridging carbonyl region is unclear, and could also arise from overtones and/or combinations.[5,6] The IR spectrum of $[Fe_3(CO)_{12}]$ in an argon matrix at 20 K is consistent with the bridged solid-state structure, and it was concluded that its structure in solution and the matrix are different.[7] A more recent IR study came to the conclusion that in solution $[Fe_3(CO)_{12}]$ is a mixture of bridged and unbridged species.[8] An EXAFS study has suggested that $[Fe_3(CO)_{12}]$ adopts primarily an all terminal carbonyl coordination in light petroleum solution, but there is a substantial population of bridging sites in a frozen CH_2Cl_2 solution.[9]

The solution ^{13}C NMR spectrum of $[Fe_3(CO)_{12}]$ is a singlet down to $-150°C$, providing little information on its solution structure.[10] This led to the conclusion that there is a very-low-energy dynamic process with an activation energy of less than 6 kcal mol^{-1}. It was postulated that the exchange occurs via the merry-go-round mechanism.[11] The ^{13}C NMR spectrum of $[Fe_3(CO)_{12}]$ has been measured in the solid-state, and consists of six signals in the ratio 1:1:1:1:1:1 at 31°C,[9] but becomes more complicated on cooling to $-90°C$.[6] Solid-state ^{13}C chemical shift anisotropy has been used to investigate the degree of bond asymmetry in both $[Fe_3(CO)_{12}]$[12] and $[Fe_3(CO)_{11}(PPh_3)]$.[13]

In order to understand the fluxionality of $[Fe_3(CO)_{12}]$ (**1**) in solution, substituents were introduced to try to block the fluxional pathway. Johnson and co-workers synthesized $[Fe_3(CO)_{11}L]$ [L = PMe_2Ph or $P(OR)_3$, R = Et, Pr^i or Ph].[14] They observed that at low temperature each compound gave rise to three ^{13}CO NMR signals, and it was believed that the intensity ratio is 6:4:1. On warming, two signals exchange to give two broad signals in the ratio 10:1 at room temperature. They ration-

* Dedicated to Prof. E. W. Abel on his retirement.

† Author to whom correspondence should be addressed.

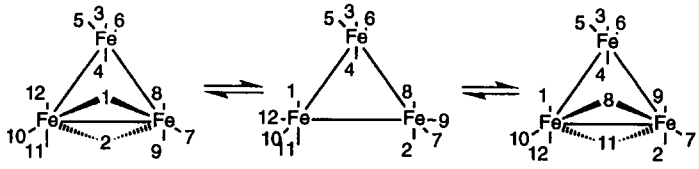

Scheme 1. The Cotton merry-go-round mechanism as applied to $[Fe_3(CO)_{12}]$, with the carbonyls represented by numbers. The mechanism shown exchanges the carbonyls $1 \leftrightarrow 12 \leftrightarrow 11 \leftrightarrow 2 \leftrightarrow 9 \leftrightarrow 8$. Exchange of the other carbonyls is achieved by bridge closure about the other Fe—Fe edges.

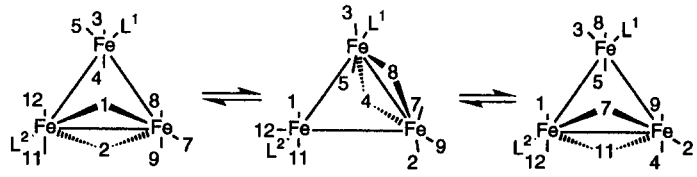

Scheme 2. The concerted bridge-opening bridge-closing mechanism as applied to $[Fe_3(CO)_{11}\{P(OMe)_3\}]$, $L^1 = C^6O$, $L^2 = P(OMe)_3$, with the carbonyls represented by numbers. The mechanism exchanges the carbonyls $1 \leftrightarrow 12 \leftrightarrow 11 \leftrightarrow 2 \leftrightarrow 7$ and $8 \leftrightarrow 3 \leftrightarrow 5 \leftrightarrow 4 \leftrightarrow 9$.

alized these observations in terms of an icosahedron ↔ cube octahedron ↔ icosahedron rearrangement, which is their description of the familiar Cotton merry-go-round mechanism, giving rise to the signal of intensity 6 (see Scheme 1).* The signal of intensity 4 arose from a trigonal twist mechanism at the unbridged iron atom. This was improbable, as such trigonal twists usually have an activation energy higher than the <7 kcal mol^{-1} required by the observation of an averaged signal.[11] Subsequently, it was shown that the actual intensities for $[Fe_3(CO)_{11}\{P(OR)_3\}]$ [R = Me, Pr^i (**2**), $L^1 = C(6)C$, $L^2 = P(OR)_3$] are 5 : 5 : 1, and that the very low energy dynamic pathway was the previously unknown concerted bridge-opening bridge-closing mechanism (see Scheme 2).[15] This mechanism exchanges carbonyls $1 \leftrightarrow 12 \leftrightarrow 11 \leftrightarrow 2 \leftrightarrow 7$ and $8 \leftrightarrow 3 \leftrightarrow 5 \leftrightarrow 4 \leftrightarrow 9$, leaving carbonyl, C(6)O, unaffected. This was later translated into the equivalent description of Johnson based on the icosahedron model.[16] It was shown that the merry-go-round mechanism begins above -100°C, with a $\Delta G\ddagger$ of 9–10 kcal mol^{-1}.[15]

Farrar and Lunniss examined $[Fe_3(CO)_{10}\{P(OMe)_3\}_2]$ and $[Fe_3(CO)_{10}\{P(OMe)_3\}\{P(OPh)_3\}]$ and showed that both compounds consist of mixtures of isomers.[17] They attempted to explain the temperature dependence of the ^{13}C NMR spectra of $[Fe_3(CO)_{10}\{P(OMe)_3\}_2]$ in terms of a very low energy merry-go-round mechanism for one isomer, and a merry-go-round mechanism with $\Delta G^\ddagger \approx 10$ kcal mol^{-1} for the other isomer. The spectra were subsequently reinterpreted in terms of the very low energy concerted bridge-opening bridge-closing mechanism, which is fast even at -100°C, and the merry-go-round mechanism becomes significant on the NMR timescale above -100°C, with a $\Delta G^\ddagger \approx 10$ kcal mol^{-1}.[18]

In 1991, Lentz showed that a limiting low temperature ^{13}C NMR spectrum is obtained from $[Fe_3(CO)_{10}L(\mu\text{-}CNCF_3)]$, L = CO, PMe_3, PEt_3, $P(OMe)_3$, $P(OEt)_3$, and CNBu^t, at -100°C,[19] and interpreted the mechanism in terms of the Johnson representation based on an icosahedron. This was claimed to be a new mechanism, but subsequently it was shown that it is the previously published concerted bridge-opening bridge-closing mechanism.[20] Johnson then translated this back into the icosahedral model, and by choosing a modified pathway which had been anticipated,[20] reduced the number of steps necessary to produce the observed exchange mechanism.[21] In the case of

*The Johnson description only differs from the Cotton description in its viewpoint. Cotton chose to use the familiar ball and stick representation of $[Fe_3(CO)_{12}]$ and moved the carbonyls around a fixed iron triangle. Johnson views the molecule as a polyhedron of ligands with a mobile iron triangle inside. Mechanistically, the two descriptions can produce identical descriptions of the mechanisms, and as the Cotton description is far easier to follow, it is this description that is used throughout this paper. The representations in this paper can be converted to those of Johnson simply by placing a dot for each ligand and joining the dots.

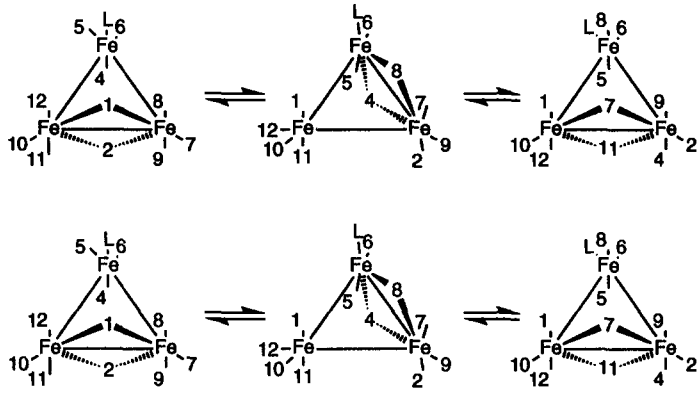

Scheme 3. The concerted bridge-opening bridge-closing mechanism applied to $[Fe_3(CO)_{11}(CNBu^t)]$, with the carbonyl ligands represented by numbers. (a) Allowing the Bu^tNC to move into an equatorial position. The dynamic process then continues to move to an axial position on an unbridged iron below the iron triangle. The exchange pathway has been established by the generation of a plane of symmetry. (b) Allowing the Bu^tNC to move into a bridging position. Both mechanisms result in the carbonyl exchange sequences $1 \leftrightarrow 8 \leftrightarrow 6 \leftrightarrow 5 \leftrightarrow 12$ and $4 \leftrightarrow 11 \leftrightarrow 10 \leftrightarrow 7 \leftrightarrow 9$, with carbonyl 2 remaining unique.

$[Fe_3(CO)_{10}L(\mu\text{-}CNCF_3)]$, $\Delta G^{\ddagger}$ for the concerted bridge-opening bridge-closing mechanism had been increased to a value accessible by variable temperature NMR spectroscopy by the strong preference of the $CNCF_3$ ligand for the bridging position.

In order to test the concerted bridge-opening bridge-closing mechanism further, two $CNBu^t$ derivatives of $[Fe_3(CO)_{12}]$ have been synthesized and examined by variable temperature NMR spectroscopy.

RESULTS AND DISCUSSION

$[Fe_3(CO)_{11}(CNBu^t)]$

The X-ray structure of $[Fe_3(CO)_{11}(CNBu^t)]$ (**3**) has been published.[22] The carbonyl region of the ^{13}C NMR spectrum at $-82°C$ is shown in Fig. 1. It consists of three signals with the approximate intensity ratio 1 : 5 : 5, at δ 242.4, 215.6 and 207.6. The observation of these three signals is consistent with a very fast concerted bridge-opening bridge-closing mechanism occurring (see Scheme 3). There are two plausible pathways available, one requires the $CNBu^t$ ligand to move into an equatorial position (see Scheme 3a) and the other requires it to transfer to a second iron atom (see Scheme 3a). Little is known about the energy difference between an axial and bridging Bu^tNC group in this system. However, it may be assumed that an equatorial Bu^tNC group is not strongly disfavoured, as the X-ray structure of $[Fe_3(CO)_{10}(CNBu^t)_2]$ shows both

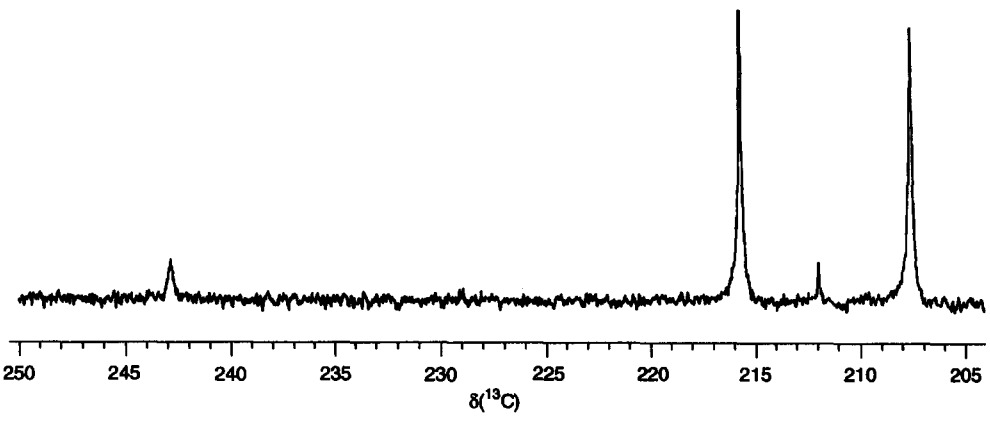

Fig. 1. The 100.62 MHz ^{13}C NMR spectrum of the carbonyl region of $[Fe_3(CO)_{11}(CNBu^t)]$ at $-82°C$ in CD_2Cl_2. The signal at δ 212 is due to an impurity.

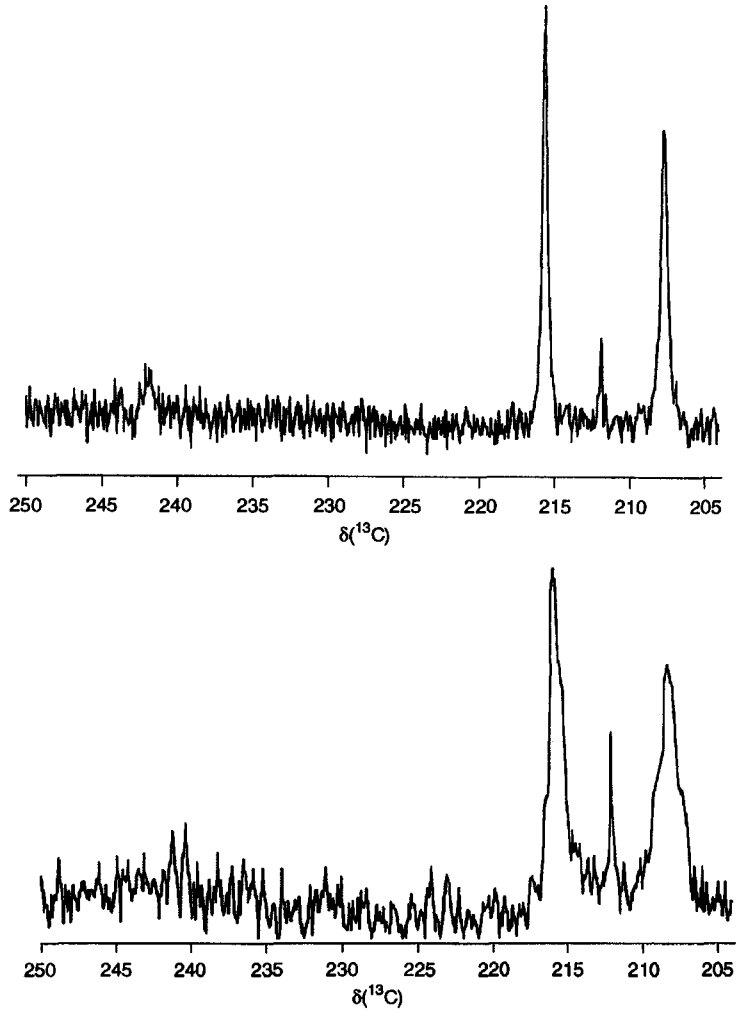

Fig. 2. The 100.62 MHz ^{13}C NMR spectrum of the carbonyl region of $[Fe_3(CO)_{11}\{P(OMe)_3\}]$ at $-72°C$ (a) and $-63°C$ (b) in CD_2Cl_2. The signal at δ 212 is due to an impurity.

$CNBu^t$ groups on the unbridged iron atom, one being axial and the other being equatorial.[23] Both mechanisms result in the exchange of carbonyls to give two sets of five carbonyls, $\overline{1 \leftrightarrow 8 \leftrightarrow 6 \leftrightarrow 5 \leftrightarrow 12}$ and $\overline{4 \leftrightarrow 11 \leftrightarrow 10 \leftrightarrow 7 \leftrightarrow 9}$, and a unique one, C(2)O.

The observed ^{13}C chemical shifts are consistent with the predominant species in solution being the same as in the solid state. The unique carbonyl has a chemical shift of δ 242.4. However, this chemical shift is significantly different from the *ca* δ 252 that would be expected for a bridging carbonyl and suggests that there is a significant concentration of at least a second species, where C(2)O is not in a bridging position. The ^{13}CN signal is at δ 152.5, which indicates no substantial contribution from an isomer with a bridging isonitrile group. As the set of carbonyls, 1, 5, 6, 8 and 12 contain a bridging carbonyl, it is to be expected that their average chemical shift will be to a higher frequency than the second set, 4, 7, 9, 10 and 11. Consequently the set of carbonyls, 1, 5, 6, 8 and 12 is assigned to the signal at δ 215.8 and the set of carbonyls, 4, 7, 9, 10, 11 is assigned to the signal at δ 207.8.

On warming from $-82°C$, all the ^{13}C NMR carbonyl signals broaden, but the signal at δ 207.6 broadens more than the signal at δ 215.6 (see Fig. 2). This is consistent with the onset of the merry-go-round mechanism exchanging carbonyls $\overline{1 \leftrightarrow 8 \leftrightarrow 9 \leftrightarrow 2 \leftrightarrow 11 \leftrightarrow 12}$, when only carbonyls 8 or 12 leave their set once for each merry-go-round shift, while carbonyls 9 and 11 both leave their set. Hence the ^{13}C NMR signal due to the set of carbonyls, 1, 5, 6, 8 and 12 should broaden at half the rate of the set of carbonyls, 4, 7, 9, 10 and 11, and this is approximately as is observed. After making allowance for only one carbonyl leaving

Fig. 3. The 162 MHz ^{31}P NMR spectrum of $[Fe_3(CO)_{10}(CNBu^t)\{P(OMe)_3\}]$ in CD_2Cl_2 at $-92°C$. The sample is known to contain a small quantity of $[Fe_3(CO)_{11}\{P(OMe)_3\}]$, producing the sharp singlet at δ 157.9. The weak signals at δ 158.6 and 162.2 may be impurities or isomers of $[Fe_3(CO)_{10}(CNBu^t)\{P(OMe)_3\}]$.

δ 215.6 and two leaving δ 207.6, the calculated activation energy for merry-go-round is 10.2 kcal mol^{-1}. At room temperature all the carbonyl signals average to give a broad ^{13}CO NMR signal at δ 215.0.

$[Fe_3(CO)_{10}(CNBu^t)\{P(OMe)_3\}]$

The ^{31}P NMR spectrum of $[Fe_3(CO)_{10}(CNBu^t)\{P(OMe)_3\}]$ is broad at room temperature, but on cooling to $-92°C$, two signals are observed in the ratio of 0.18:1 at δ 166.0 and 159.3 (see Fig. 3). The ^{13}C NMR spectrum shows a carbonyl spectrum at $-92°C$, which has six strong signals due to the major isomer with approximate intensities 1:2:2:2:2:1 at δ 249.0, 231.5, 214.9, 211.5, 209.3 and 207.2. The isonitrile carbon NMR signals are at δ 152.8 (major isomer) and 155.3 (minor isomer). The isonitrile ^{13}C NMR signal of the minor isomer shows $J(^{31}P^{13}C) = 30$ Hz (see Fig. 4).

The X-ray structure of $[Fe_3(CO)_{10}(CNBu^t)\{P(OMe)_3\}]$

In order to provide some evidence of one of the isomers present in $[Fe_3(CO)_{10}(CNBu^t)\{P(OMe)_3\}]$, the crystal structure was determined. The crystal contains two independent molecules in the unit cell, and one is illustrated in Fig. 5. Bond lengths and bond angles are given in Table 1 and the atom coordinates in Table 2.

The X-ray structure is comparable with those reported previously for other $[Fe_3(CO)_{12}]$ derivatives of $P(OR)_3$ and $CNBu^t$. The $P(OMe)_3$ group lies in an equatorial position attached to one of the iron atoms involved in the carbonyl bridge. The Fe–P lengths of 2.171(3) and 2.174(3) Å for the two independent molecules in the unit cell are similar to those observed for $[Fe_3(CO)_{10}(\mu\text{-}CNCF_3)\{P(OMe)_3\}]$ of 2.172(3),[19] and $[Fe_3(CO)_{10}\{P(OMe)_3\}_2]$, of 2.166(5) and 2.270(19) Å,[11] for a $P(OMe)_3$ ligand on an iron atom with bridging carbonyl ligands. The $CNBu^t$ ligand is in the axial

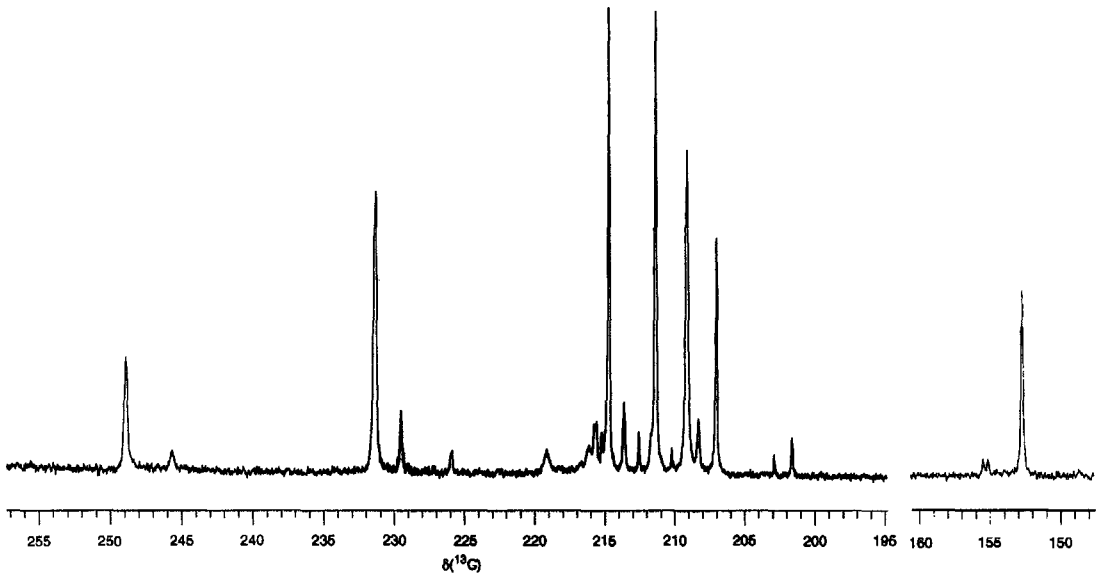

Fig. 4. The 100.62 MHz ^{13}C NMR spectrum of $[Fe_3(CO)_{10}(CNBu^t)\{P(OMe)_3\}]$ in CD_2Cl_2 at $-92°C$. The sample is known to contain a small quantity of $[Fe_3(CO)_{11}\{P(OMe)_3\}]$, producing the signals at δ 219.2, 216.2 and 203.0.

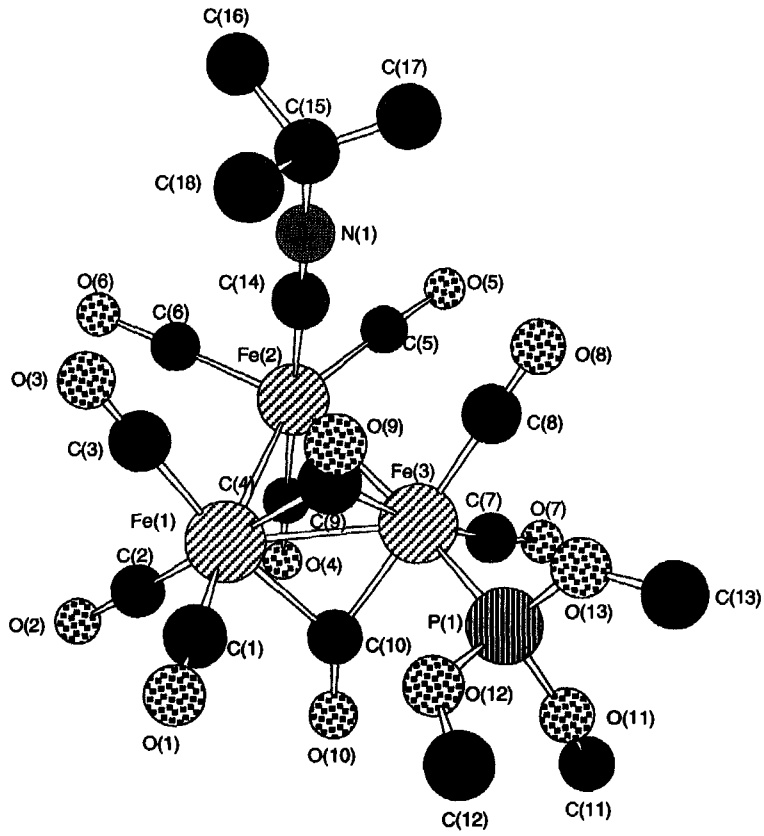

Fig. 5. The X-ray structure of one isomer of $[Fe_3(CO)_{10}(CNBu^t)\{P(OMe)_3\}]$.

position on the unbridged iron, as has been previously observed for $[Fe_3(CO)_{11}(CNBu^t)]$.[18] The Fe–CN bond lengths of 1.892(9) and 1.882(9) Å are similar to that observed for $[Fe_3(CO)_{11}(CNBu^t)]$ of 1.909(5) and $[Fe_3(CO)_{10}(CNBu^t)_2]$ of 1.902(1) (axial) and 1.856(8) (equatorial). The bridging carbonyls are not in the centre of the bridge, with the distances Fe(1)–C(9) = 1.975(9) Å, Fe(1)–

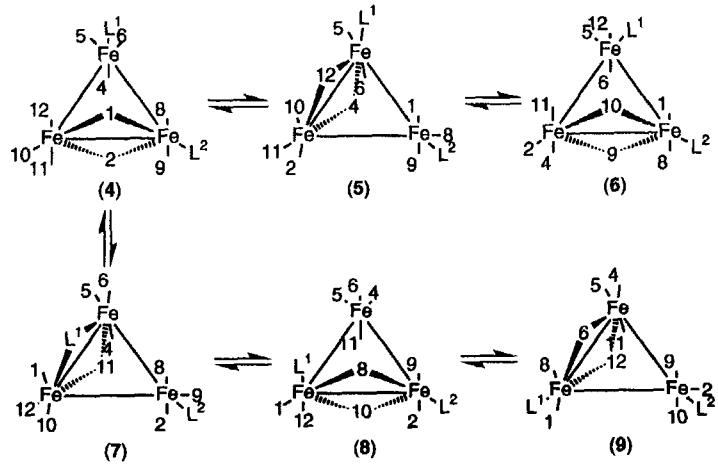

Scheme 4. The concerted bridge-opening bridge-closing mechanism applied to $[Fe_3(CO)_{10}(CNBu^t)\{P(OMe)_3\}]$, $L^1 = CNBu^t$, $L^2 = P(OMe)_3$, with the carbonyl ligands represented by numbers. After allowing the Bu^tNC to move into an equatorial position, the dynamic process continues moving the Bu^tNC to an axial position on an unbridged iron below the iron triangle. The exchange pathway has been established by the generation of a plane of symmetry.

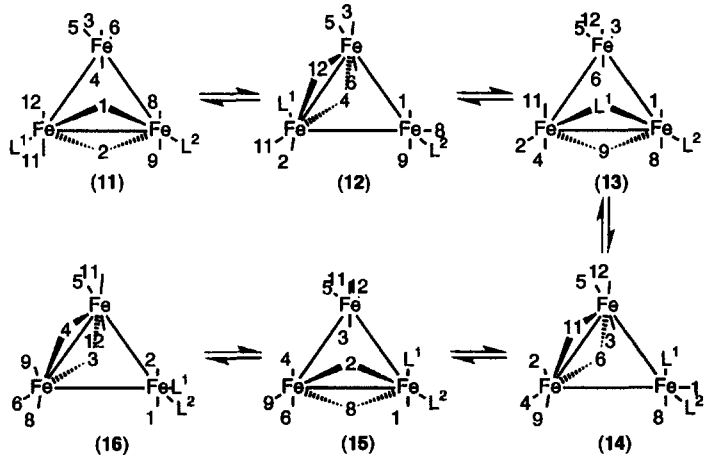

Scheme 5. The concerted bridge-opening bridge-closing mechanism applied to $[Fe_3(CO)_{10}(CNBu^t)\{P(OMe)_3\}]$, $L^1 = CNBu^t$, $L^2 = P(OMe)_3$, with the carbonyl ligands represented by numbers. After allowing the Bu^tNC to move into an equatorial position, the dynamic process continues moving the Bu^tNC to an axial position on an unbridged iron below the iron triangle. The exchange pathway has been established by the generation of a plane of symmetry.

C(10) = 2.066(8) Å, Fe(3)–C(9) = 1.998(9) Å and Fe(3)–C(10) = 1.933(9) Å. There is a corresponding positioning of terminal carbonyls towards bridging the Fe(1)–Fe(2) edge, with the distances Fe(1)–C(4) = 3.131 Å, Fe(1)–C(14) = 3.315 Å, Fe(2)–C(2) = 3.250 Å, Fe(2)–C(3) = 3.106 Å, Fe(2)–C(7) = 3.180 Å, Fe(2)–C(8) = 3.211 Å, Fe(3)–C(4) = 3.146 Å and Fe(3)–C(14) = 3.211 Å. This positioning shows that the structure is intermediate between the symmetric bridged structure and the transition state required by the concerted bridge-opening bridge-closing mechanism.[15]

The solution structure of $[Fe_3(CO)_{10}(CNBu^t)\{P(OMe)_3\}]$.

In the following discussion it will be assumed that at low temperature the $P(OMe)_3$ ligand remains in an equatorial position. In order to account for the dynamic ^{13}C NMR spectrum of $[Fe_3(CO)_{11}\{P(OMe)_3\}]$, moving the $P(OMe)_3$ ligand to an axial position is requires at least 13.0 kcal mol^{-1}, otherwise the unique carbonyl would exchange at a lower energy.[11] The ^{13}C NMR spectrum of the major isomer at $-92°C$ fits the structure found in the crystal structure, provided that the concerted bridge-opening bridge-closing mechanism is occurring very fast on the NMR timescale. This is shown in Scheme 4.

The dynamic pathway, for (**4**) in Scheme 4 results in the pairwise exchanges of C(1)O and C(8)O, C(4)O and C(11)O, C(6)O and C(12)O, and C(9)O and C(10)O, leaving C(2)O and C(5)O unaffected. This would give rise to the observed 1:2:2:2:2:1 intensity pattern for the ^{13}CO signals at $-92°C$. The same could be said for any of the other isomers which can reach (**4**) by the concerted bridge-opening bridge-closing mechanism. This includes (**5**), (**6**), (**7**), (**8**), and (**9**). Carbonyl C(2)O is bridging in isomer (**4**), and the minor isomer has a signal at δ 245.7, while the major isomer has a signal at δ 249.0 of intensity 1. None of the other isomers in Scheme 4 has the unique carbonyls C(2)O or C(5)O in a bridging position. This is consistent with one of the isomers present being (**4**), as is found in the crystal structure.

There are two other families of isomers possible, (**10**), and a family of structures, (**11**)–(**16**), interrelated by the concerted bridge-opening bridge-closing mechanism, see Scheme 5.

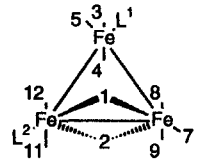

In (**10**), $L^1 = CNBu^t$, $L^2 = P(OMe)_3$ or $L^1 = P(OMe)_3$, $L^2 = CNBu^t$. The dynamic pathway via the concerted bridge-opening bridge-closing mechanism is available as shown in Scheme 2, and two sets of ^{13}CO signals will be observed with equal populations, 5:5. This can be ruled out as the major species, which gives carbonyl intensities 1:2:2:2:2:1.

The third group of structures and their interconversion by the concerted bridge-opening bridge-closing mechanism is shown in Scheme 5. Structures (**11**) and (**16**) possess a plane of symmetry, and it

Table 1. Selected bond lengths (Å) and angles (°) in the complex $[Fe_3(CO)_{10}(CNBu^t)\{P(OMe)_3\}]$

Fe(1)—C(1)	1.775(10)	Fe(2a)—C(5a)	1.799(10)	O(11)—C(11)	1.301(12)
Fe(1)—C(3)	1.806(10)	Fe(2a)—C(14a)	1.882(9)	O(12)—C(12)	1.368(12)
Fe(1)—C(2)	1.812(10)	Fe(2a)—Fe(3a)	2.694(2)	O(13)—C(13)	1.360(13)
Fe(1)—C(9)	1.975(9)	Fe(3a)—C(8a)	1.774(11)	C(15)—C(17)	1.33(2)
Fe(1)—C(10)	2.066(8)	Fe(3a)—C(7a)	1.793(11)	C(15)—C(18)	1.35(2)
Fe(1)—Fe(3)	2.548(2)	Fe(3a)—C(10a)	1.954(9)	C(15)—C(16)	1.39(2)
Fe(1)—Fe(2)	2.693(2)	Fe(3a)—C(9a)	1.982(9)	O(1a)—C(1a)	1.138(10)
Fe(2)—C(5)	1.793(10)	Fe(3a)—P(1a)	2.174(3)	O(2a)—C(2a)	1.116(10)
Fe(2)—C(4)	1.797(10)	P(1)—O(11)	1.507(8)	O(3a)—C(3a)	1.157(10)
Fe(2)—C(6)	1.806(10)	P(1)—O(12)	1.548(8)	O(4a)—C(4a)	1.145(10)
Fe(2)—C(14)	1.892(9)	P(1)—O(13)	1.550(8)	O(5a)—C(5a)	1.135(10)
Fe(2)—Fe(3)	2.696(2)	P(1a)—O(11a)	1.534(9)	O(6a)—C(6a)	1.147(9)
Fe(3)—C(7)	1.783(10)	P(1a)—O(12a)	1.570(7)	O(7a)—C(7a)	1.135(10)
Fe(3)—C(8)	1.794(9)	P(1a)—O(13a)	1.627(9)	O(8a)—C(8a)	1.161(10)
Fe(3)—C(10)	1.933(9)	N(1)—C(14)	1.147(9)	O(9a)—C(9a)	1.162(9)
Fe(3)—C(9)	1.998(9)	N(1)—C(15)	1.449(11)	O(10a)—C(10a)	1.168(9)
Fe(3)—P(1)	2.171(3)	O(1)—C(1)	1.139(10)	O(11a)—C(11a)	1.40(2)
Fe(1a)—C(3a)	1.778(11)	O(2)—C(2)	1.137(10)	O(12a)—C(12a)	1.434(11)
Fe(1a)—C(1a)	1.789(11)	O(3)—C(3)	1.139(10)	O(13a)—C(13a)	1.271(13)
Fe(1a)—C(2a)	1.834(10)	O(4)—C(4)	1.154(9)	N(1a)—C(14a)	1.164(10)
Fe(1a)—C(9a)	2.010(9)	O(5)—C(5)	1.141(10)	N(1a)—C(15a)	1.444(12)
Fe(1a)—C(10a)	2.029(10)	O(6)—C(6)	1.124(10)	C(15a)—C(17a)	1.34(2)
Fe(1a)—Fe(3a)	2.548(2)	O(7)—C(7)	1.150(10)	C(15a)—C(16a)	1.34(2)
Fe(1a)—Fe(2a)	2.695(2)	O(8)—C(8)	1.130(9)	C(15a)—C(18a)	1.48(2)
Fe(2a)—C(4a)	1.784(10)	O(9)—C(9)	1.169(9)		
Fe(2a)—C(6a)	1.793(10)	O(10)—C(10)	1.152(8)		

C(1)—Fe(1)—C(3)	98.6(4)	C(3)—Fe(1)—Fe(3)	124.9(3)
C(1)—Fe(1)—C(2)	95.6(4)	C(2)—Fe(1)—Fe(3)	124.3(3)
C(3)—Fe(1)—C(2)	95.3(4)	C(9)—Fe(1)—Fe(3)	50.5(3)
C(1)—Fe(1)—C(9)	90.1(4)	C(10)—Fe(1)—Fe(3)	48.2(2)
C(3)—Fe(1)—C(9)	86.4(3)	C(1)—Fe(1)—Fe(2)	173.4(3)
C(2)—Fe(1)—C(9)	173.7(4)	C(3)—Fe(1)—Fe(2)	84.2(3)
C(1)—Fe(1)—C(10)	91.9(4)	C(2)—Fe(1)—Fe(2)	90.1(3)
C(3)—Fe(1)—C(10)	169.4(4)	C(9)—Fe(1)—Fe(2)	84.0(2)
C(2)—Fe(1)—C(10)	85.3(4)	C(10)—Fe(1)—Fe(2)	85.2(2)
C(9)—Fe(1)—C(10)	91.8(3)	Fe(3)—Fe(1)—Fe(2)	61.84(4)
C(1)—Fe(1)—Fe(3)	112.0(3)	C(5)—Fe(2)—C(4)	91.6(4)
C(5)—Fe(2)—C(6)	101.9(4)	C(2a)—Fe(1a)—C(9a)	172.7(4)
C(4)—Fe(2)—C(6)	91.0(4)	C(3a)—Fe(1a)—C(10a)	171.0(4)
C(5)—Fe(2)—C(14)	91.1(4)	C(1a)—Fe(1a)—C(10a)	91.8(4)
C(4)—Fe(2)—C(14)	176.2(4)	C(2a)—Fe(1a)—C(10a)	85.2(4)
C(6)—Fe(2)—C(14)	91.1(3)	C(9a)—Fe(1a)—C(10a)	92.1(4)
C(5)—Fe(2)—Fe(1)	156.6(3)	C(3a)—Fe(1a)—Fe(3a)	125.9(3)
C(4)—Fe(2)—Fe(1)	85.5(3)	C(1a)—Fe(1a)—Fe(3a)	112.0(3)
C(6)—Fe(2)—Fe(1)	101.3(3)	C(2a)—Fe(1a)—Fe(3a)	124.5(3)
C(14)—Fe(2)—Fe(1)	90.9(2)	C(9a)—Fe(1a)—Fe(3a)	49.8(3)
C(5)—Fe(2)—Fe(3)	100.2(3)	C(10a)—Fe(1a)—Fe(3a)	48.9(3)
C(4)—Fe(2)—Fe(3)	87.1(3)	C(3a)—Fe(1a)—Fe(2a)	84.0(3)
C(6)—Fe(2)—Fe(3)	157.8(3)	C(1a)—Fe(1a)—Fe(2a)	172.3(3)
C(14)—Fe(2)—Fe(3)	89.8(2)	C(2a)—Fe(1a)—Fe(2a)	91.2(3)
Fe(1)—Fe(2)—Fe(3)	56.44(4)	C(9a)—Fe(1a)—Fe(2a)	81.9(2)
C(7)—Fe(3)—C(8)	91.1(4)	C(10a)—Fe(1a)—Fe(2a)	87.0(2)
C(7)—Fe(3)—C(10)	89.7(4)	Fe(3a)—Fe(1a)—Fe(2a)	61.77(5)
C(8)—Fe(3)—C(10)	176.7(4)	C(4a)—Fe(2a)—C(6a)	91.7(4)
C(7)—Fe(3)—C(9)	169.0(4)	C(4a)—Fe(2a)—C(5a)	101.9(4)
C(8)—Fe(3)—C(9)	83.5(3)	C(6a)—Fe(2a)—C(5a)	92.9(4)
C(10)—Fe(3)—C(9)	95.2(3)	C(4a)—Fe(2a)—C(14a)	91.3(4)

Table 1—*continued.*

C(7)—Fe(3)—P(1)	99.1(3)	C(6a)—Fe(2a)—C(14a)	175.9(4)
C(8)—Fe(3)—P(1)	93.1(3)	C(5a)—Fe(2a)—C(14a)	89.2(4)
C(10)—Fe(3)—P(1)	89.9(3)	C(4a)—Fe(2a)—Fe(3a)	156.9(3)
C(9)—Fe(3)—P(1)	90.8(2)	C(6a)—Fe(2a)—Fe(3a)	84.9(3)
C(7)—Fe(3)—Fe(1)	128.8(3)	C(5a)—Fe(2a)—Fe(3a)	101.1(3)
C(8)—Fe(3)—Fe(1)	124.6(3)	C(14a)—Fe(2a)—Fe(3a)	91.2(2)
C(10)—Fe(3)—Fe(1)	52.8(2)	C(4a)—Fe(2a)—Fe(1a)	100.6(3)
C(9)—Fe(3)—Fe(1)	49.7(2)	C(6a)—Fe(2a)—Fe(1a)	86.1(3)
P(1)—Fe(3)—Fe(1)	112.29(9)	C(5a)—Fe(2a)—Fe(1a)	157.5(3)
C(7)—Fe(3)—Fe(2)	86.8(3)	C(14a)—Fe(2a)—Fe(1a)	90.7(2)
C(8)—Fe(3)—Fe(2)	89.1(3)	Fe(3a)—Fe(2a)—Fe(1a)	56.44(4)
C(10)—Fe(3)—Fe(2)	87.8(2)	C(8a)—Fe(3a)—C(7a)	93.2(4)
C(9)—Fe(3)—Fe(2)	83.5(2)	C(8a)—Fe(3a)—C(10a)	84.9(4)
P(1)—Fe(3)—Fe(2)	173.64(9)	C(7a)—Fe(3a)—C(10a)	173.3(4)
Fe(1)—Fe(3)—Fe(2)	61.72(4)	C(8a)—Fe(3a)—C(9a)	173.3(4)
C(3a)—Fe(1a)—C(1a)	97.2(4)	C(7a)—Fe(3a)—C(9a)	85.8(4)
C(3a)—Fe(1a)—C(2a)	94.4(4)	C(10a)—Fe(3a)—C(9a)	95.2(4)
C(1a)—Fe(1a)—C(2a)	96.3(4)	C(8a)—Fe(3a)—P(1a)	97.4(3)
C(3a)—Fe(1a)—C(9a)	87.3(4)	C(7a)—Fe(3a)—P(1a)	97.0(3)
C(1a)—Fe(1a)—C(9a)	90.5(4)	C(10a)—Fe(3a)—P(1a)t	89.7(3)
C(9a)—Fe(3a)—P(1a)	89.4(3)	O(10)—C(10)—Fe(1)	135.7(7)
C(8a)—Fe(3a)—Fe(1a)	125.9(3)	Fe(3)—C(10)—Fe(1)	79.1(3)
C(7a)—Fe(3a)—Fe(1a)	126.0(3)	N(1)—C(14)—Fe(2)	174.0(7)
C(10a)—Fe(3a)—Fe(1a)	51.5(3)	C(17)—C(15)—C(18)	111(2)
C(9a)—Fe(3a)—Fe(1a)	50.8(2)	C(17)—C(15)—C(16)	106(2)
P(1a)—Fe(3a)—Fe(1a)	110.83(9)	C(18)—C(15)—C(16)	110(2)
C(8a)—Fe(3a)—Fe(2a)	90.9(3)	C(17)—C(15)—N(1)	109.2(11)
C(7a)—Fe(3a)—Fe(2a)	85.0(3)	C(18)—C(15)—N(1)	111.2(10)
C(10a)—Fe(3a)—Fe(2a)	88.6(3)	C(16)—C(15)—N(1)	110.7(9)
C(9a)—Fe(3a)—Fe(2a)	82.4(2)	C(11a)—O(11a)—P(1a)	119.2(10)
P(1a)—Fe(3a)—Fe(2a)	171.39(10)	C(12a)—O(12a)—P(1a)	124.0(7)
Fe(1a)—Fe(3a)—Fe(2a)	61.79(5)	C(13a)—O(13a)—P(1a)	128.3(12)
O(11)—P(1)—O(12)	102.3(6)	C(14a)—N(1a)—C(15a)	177.4(10)
O(11)—P(1)—O(13)	100.1(6)	O(1a)—C(1a)—Fe(1a)	179.2(10)
O(12)—P(1)—O(13)	104.9(6)	O(2a)—C(2a)—Fe(1a)	176.0(9)
O(11)—P(1)—Fe(3)	122.9(4)	O(3a)—C(3a)—Fe(1a)	176.7(9)
O(12)—P(1)—Fe(3)	111.9(3)	O(4a)—C(4a)—Fe(2a)	178.7(8)
O(13)—P(1)—Fe(3)	112.8(3)	O(5a)—C(5a)—Fe(2a)	178.9(9)
O(11a)—P(1a)—O(12a)	107.3(5)	O(6a)—C(6a)—Fe(2a)	173.4(8)
O(11a)—P(1a)—O(13a)	97.5(6)	O(7a)—C(7a)—Fe(3a)	176.6(10)
O(12a)—P(1a)—O(13a)	98.6(5)	O(8a)—C(8a)—Fe(3a)	178.8(9)
O(11a)—P(1a)—Fe(3a)	121.6(4)	O(9a)—C(9a)—Fe(3a)	142.5(7)
O(12a)—P(1a)—Fe(3a)	112.0(3)	O(9a)—C(9a)—Fe(1a)	138.2(7)
O(13a)—P(1a)—Fe(3a)	116.7(4)	Fe(3a)—C(9a)—Fe(1a)	79.3(4)
C(14)—N(1)—C(15)	177.9(9)	O(10a)—C(10a)—Fe(3a)	143.7(8)
C(11)—O(11)—P(1)	139.8(9)	O(10a)—C(10a)—Fe(1a)	136.7(7)
C(12)—O(12)—P(1)	130.5(9)	Fe(3a)—C(10a)—Fe(1a)	79.5(4)
C(13)—O(13)—P(1)	133.7(10)	N(1a)—C(14a)—Fe(2a)	174.4(7)
O(1)—C(1)—Fe(1)	179.5(10)	C(17a)—C(15a)—C(16a)	111(2)
O(2)—C(2)—Fe(1)	175.8(8)	C(17a)—C(15a)—N(1a)	113.4(12)
O(3)—C(3)—Fe(1)	177.6(9)	C(16a)—C(15a)—N(1a)	108.0(11)
O(4)—C(4)—Fe(2)	175.4(8)	C(17a)—C(15a)—C(18a)	110.8(14)
O(5)—C(5)—Fe(2)	178.5(9)	C(16a)—C(15a)—C(18a)	107(2)
O(6)—C(6)—Fe(2)	178.3(9)	N(1a)—C(15a)—C(18a)	105.8(10)
O(7)—C(7)—Fe(3)	176.2(8)		
O(8)—C(8)—Fe(3)	177.5(8)		
O(9)—C(9)—Fe(1)	140.3(7)		
O(9)—C(9)—Fe(3)	139.9(7)		
Fe(1)—C(9)—Fe(3)	79.8(3)		
O(10)—C(10)—Fe(3)	145.2(7)		

Table 2. Atom coordinates ($\times 10^4$)

Atom	x	y	z	U_{eq}
Fe(1)	3349(1)	−457(1)	2521(1)	57(1)
Fe(2)	1099(1)	−315(1)	2707(1)	52(1)
Fe(3)	2291(1)	257(1)	1857(1)	54(1)
Fe(1a)	1797(1)	2099(1)	7461(1)	61(1)
Fe(2a)	4157(1)	2182(1)	7616(1)	56(1)
Fe(3a)	2847(1)	2672(1)	8511(1)	62(1)
P(1)	3428(2)	684(1)	1249(1)	73(1)
P(1a)	1583(3)	3063(1)	9071(2)	89(1)
N(1)	1818(6)	242(2)	4272(4)	65(2)
O(1)	5796(7)	−498(3)	2283(5)	119(3)
O(2)	2817(6)	−1419(2)	2014(5)	107(2)
O(3)	3775(6)	−665(3)	4296(4)	100(2)
O(4)	388(6)	−854(2)	1185(4)	90(2)
O(5)	−1211(7)	142(3)	2428(5)	114(3)
O(6)	707(7)	−1124(2)	3688(5)	102(2)
O(7)	104(6)	333(2)	649(4)	94(2)
O(8)	1573(6)	1044(2)	2761(4)	96(2)
O(9)	4133(5)	430(2)	3343(4)	75(2)
O(10)	2785(6)	−450(2)	676(4)	85(2)
O(11)	3189(10)	774(4)	335(5)	217(7)
O(12)	4711(7)	501(3)	1391(6)	140(3)
O(13)	3529(10)	1186(3)	1577(6)	160(4)
C(1)	4838(9)	−481(3)	2373(6)	75(3)
C(2)	2985(8)	−1043(3)	2189(6)	71(2)
C(3)	3585(8)	−585(3)	3609(6)	68(2)
C(4)	710(7)	−640(3)	1770(6)	67(2)
C(5)	−313(9)	−36(3)	2547(5)	71(2)
C(6)	840(8)	−811(3)	3312(5)	68(2)
C(7)	972(9)	291(3)	1109(5)	70(2)
C(8)	1830(8)	735(3)	2415(5)	66(2)
C(9)	3558(7)	198(3)	2848(5)	58(2)
C(10)	2765(7)	−281(3)	1304(5)	60(2)
C(11)	2600(12)	598(4)	−340(6)	125(4)
C(12)	5669(11)	646(5)	1073(10)	180(7)
C(13)	3734(12)	1599(4)	1238(10)	182(7)
C(14)	1606(7)	36(3)	3671(5)	55(2)
C(15)	2129(10)	495(4)	5037(6)	85(3)
C(16)	1618(17)	293(7)	5655(8)	269(13)
C(18)	3307(15)	515(9)	5279(12)	447(30)
C(17)	1674(25)	917(6)	4939(11)	515(38)
O(1a)	−771(6)	2144(3)	7318(5)	121(3)
O(2a)	1929(6)	1085(2)	7604(4)	100(2)
O(3a)	1810(7)	2082(3)	5685(5)	109(2)
O(4a)	4639(7)	1486(3)	6432(5)	108(2)
O(5a)	6531(6)	2536(3)	8247(5)	122(3)
O(6a)	4402(6)	1486(2)	8927(4)	95(2)
O(7a)	4303(7)	3457(3)	8195(5)	122(3)
O(8a)	4464(7)	2446(3)	10042(5)	121(3)
O(9a)	1520(5)	3085(2)	6962(4)	79(2)
O(10a)	1802(6)	1861(2)	9225(4)	91(2)
O(11a)	1733(9)	3582(3)	9239(7)	156(4)
O(12a)	282(6)	2984(2)	8617(5)	106(2)
O(13a)	1420(9)	2908(3)	9993(6)	147(3)
N(1a)	3941(6)	2907(3)	6264(5)	74(2)
C(1a)	228(9)	2125(3)	7379(6)	83(3)
C(2a)	1919(8)	1470(4)	7565(6)	76(3)

Table 2.—*continued.*

Atom	*x*	*y*	*z*	U_{eq}
C(3a)	1833(8)	2097(3)	6388(7)	76(3)
C(4a)	4457(7)	1755(3)	6903(6)	66(2)
C(5a)	5608(9)	2403(3)	8004(6)	77(3)
C(6a)	4241(7)	1764(3)	8424(6)	72(2)
C(7a)	3721(8)	3154(4)	8294(6)	84(3)
C(8a)	3827(8)	2531(3)	9433(7)	78(3)
C(9a)	1881(7)	2790(3)	7413(6)	65(2)
C(10a)	2037(7)	2102(3)	8709(6)	68(2)
C(11a)	1659(14)	3887(5)	8572(10)	179(7)
C(12a)	−725(10)	3212(5)	8833(9)	151(5)
C(13a)	2061(14)	3012(6)	10677(9)	189(8)
C(14a)	3973(7)	2639(3)	6793(5)	63(2)
C(15a)	3892(11)	3255(4)	5633(7)	102(4)
C(16a)	3484(22)	3056(6)	4902(10)	511(34)
C(17a)	3242(17)	3623(6)	5760(13)	439(28)
C(18a)	5129(14)	3389(5)	5628(9)	178(7)

can easily be seen that the dynamic pathway exchanges carbonyls C(1)O and C(2)O, C(3)O and C(4)O, C(8)O and C(9)O, and C(11)O, and C(12)O. The unique carbonyls are C(5)O and C(6)O. As with (**4**), this produces six carbonyl signals with intensities 1:2:2:2:2:1. Carbonyl C(6)O is bridging in isomer (**14**), and the minor isomer has a signal at δ 245.7, while the major isomer has a signal at δ 249.0. None of the other isomers in Scheme 5 has carbonyls C(5)O or C(6)O in a bridging position. It is therefore concluded that (**14**) is the predominant isomer of the second form of $[Fe_3(CO)_{10}(CNBu^t)\{P(OMe)_3\}]$.

By analogy with the ^{13}C NMR data on $[Fe_3(CO)_{12-n}\{P(OMe)_3\}_n]$, $n = 2$ or 3,[11] $J(^{31}P^{13}C)$ to the $^{13}CNBu^t$ in (**4**) would be expected to be undetectable, while in (**14**) it would be expected to be *ca* 30–35 Hz. It is therefore concluded that the major isomer is predominantly (**4**) and the minor isomer is predominantly (**14**). It is this stereochemistry that has been reported for the crystal structure of $[Fe_3(CO)_{10}(CNBu^t)_2]$.[23]

In both cases, the bridging carbonyls ^{13}C chemical shift deviates significantly from the expected δ 252 and this could indicate that some other isomers are present at low concentration, interconverting with (**4**) and (**14**) rapidly *via* the concerted bridge-opening bridge-closing mechanism as shown in Schemes 4 and 5, respectively.

The assignment of the ^{13}CO signals of the major isomer follows from Scheme 4, their anticipated chemical shifts and $J(^{31}P^{13}C)$.[11] The signal due to C(2)O is at δ 249.0, with $J(^{31}P^{13}C) = 10$ Hz; C(1)O and C(8)O at δ 231.5, with $J(^{31}P^{13}C) = 12$ Hz;

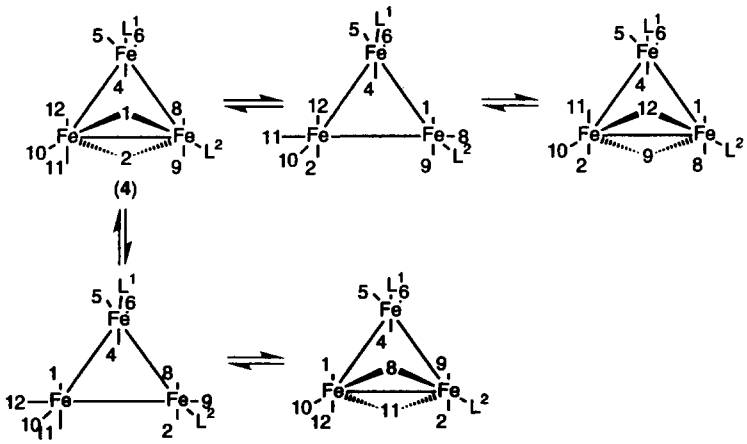

Scheme 6. The merry-go-round mechanism applied to the bridged edge of $[Fe_3(CO)_{10}(CNBu^t)\{P(OMe)_3\}]$, $L^1 = CNBu^t$, $L^2 = P(OMe)_3$, with the carbonyl ligands represented by numbers.

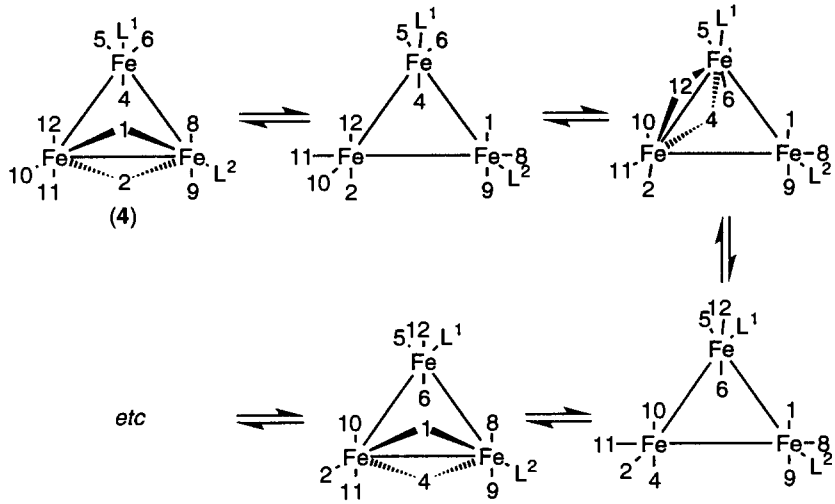

Scheme 7. The merry-go-round mechanism applied to an unbridged edge of $[Fe_3(CO)_{10}(CNBu^t)\{P(OMe)_3\}]$, $L^1 = CNBu^t$, $L^2 = P(OMe)_3$, with the carbonyl ligands represented by numbers.

C(9)O and C(10)O at 209.3, with $J(^{31}P^{13}C) = 6$ Hz; and C(5)O at δ 207.2. The relative assignment of the signals due to C(6)O and C(12)O and to C(4)O and C(11)O follows from magnetization transfer measurements. On warming the sample to $-77°C$, selective DANTE pulses were applied in turn to the signals at δ 231.5, 214.9, 209.3 and the data analysed quantitatively as previously described.[24] The magnetization transfer measurements showed that the dominant exchange pathways are δ 249.0 with δ 214.9 and 209.3, δ 231.5 with 211.5 and 209.3, δ 214.9 with 249.0 and 211.5, δ 211.5 with 231.5 and 214.9, and δ 209.3 with 249.0 and 231.5. The merry-go-round mechanism is expected to apply to these systems with an activation energy of around 10 kcal mol^{-1}. There are two such pathways, one exchanging carbonyls $\overline{1\leftrightarrow8\leftrightarrow9\leftrightarrow2\leftrightarrow11\leftrightarrow12}$, as shown in Scheme 6. The second pathway involves bridging the edge which does not contain the iron which bears the $P(OMe)_3$ (see Scheme 7). This results in the pairwise exchange C(1)O with C(4)O, C(6)O with C(12)O, C(8)O with C(9)O, and C(10)O with C(11)O. The merry-go-round mechanism is not applied to the third edge as this would involve the $P(OMe)_3$ ligand going into an axial position, and this is known to require at least 13 kcal mol^{-1}. Consequently C(5)O is not brought into the exchange at this point. This analysis results in the ex-

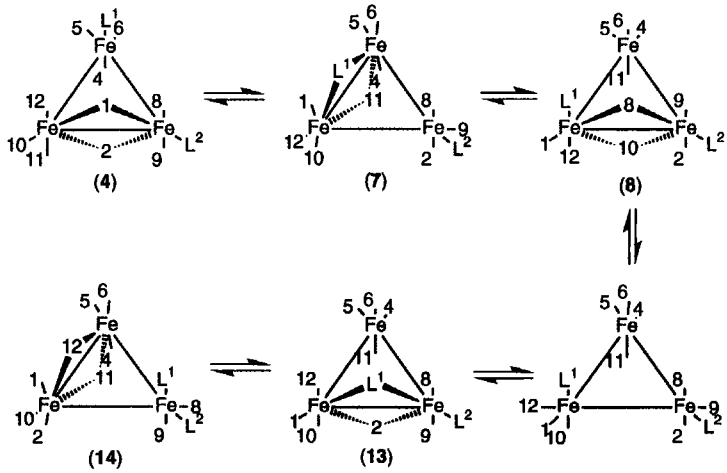

Scheme 8. A possible mechanism to interconvert the major and minor isomers of $[Fe_3(CO)_{10}(CNBu^t)\{P(OMe)_3\}]$, $L^1 = CNBu^t$, $L^2 = P(OMe)_3$.

Table 3. The exchange matrix used to fit the magnetization transfer data on $[Fe_3(CO)_{10}(CNBu^t)\{P(OMe)_3\}]$. k_1 refers to one bridge-opening bridge-closing merry-go-round step as in Scheme 6, while k_2 refers to the multiple bridge-opening bridge-closing merry-go-round steps required in Scheme 7 to move the $CNBu^t$ from above the Fe_3 plane to below the Fe_3 plane

	C(2)O δ249.0	C(1)O, C(8)O δ231.5	C(4)O, C(11)O δ214.9	C(6)O, C(12)O δ211.5	C(9)O, C(10)O δ209.3
C(2)O/δ249.0	—	0	k_1	0	k_1
C(1)O, C(8)O/δ231.5	0	—	$0.5k_2$	$0.5k_1$	$0.5(k_1+k_2)$
C(4)O, C(11)O/δ214.9	$0.5k_1$	$0.5k_2$	—	$0.5k_1$	$0.5k_2$
C(6)O, C(12)O/δ211.5	0	$0.5k_1$	$0.5k_1$	—	0
C(9)O, C(10)O/δ209.3	$0.5k_1$	$0.5(k_1+k_2)$	$0.5k_2$	0	—

change matrix shown in Table 3, and calculated rate constants k_1 of 7.5 s^{-1} and k_2 of 2.8 s^{-1} at $-77°C$, giving $\Delta G^{\ddagger} = 10.5$ and 10.9 kcal mol^{-1}, respectively.

In the major isomer, an averaged signal is observed at δ 231.5 for C(1)O and C(8)O. The chemical shift of C(1)O can be estimated as *ca* δ 250 and of C(8)O as *ca* δ 215, giving a separation of *ca* 3500 Hz at 100.62 MHz. The linewidth of this signal at $-100°C$ is *ca* 20 Hz. Using the equation $k = (\pi(v_A - v_B)^2/2\Delta v)$, where $v_A - v_B$ is the separation of the exchanging signals in Hz, and Δv is the residual line broadening, k can be estimated as 10^6 s^{-1}, leading to an estimate of $\Delta G^{\ddagger} = 5.2$ kcal mol^{-1} for the concerted bridge-opening bridge-closing mechanism. This is best viewed as an upper limit for $\Delta G^{\ddagger}$, due to difficulties in estimating the linewidth in the absence of exchange.

Interchange between the two isomers is also significant, and this was investigated by ^{31}P line shape analysis yielding $\Delta G^{\ddagger} = 10.6$ and 10.0 kcal mol^{-1} at $-57°C$ for the activation energy for converting the major isomer to the minor and *vice versa*. There are a number of possible pathways possible for this interconversion. However, due to the similarity of the activation energy to that found for the merry-go-round process, a plausible pathway is shown in Scheme 8, which involves both the very low energy concerted bridge-opening bridge-closing mechanism and one step of the merry-go-round.

A tentative assignment can be made of the ^{13}C carbonyl signals of (14), using the numbering in

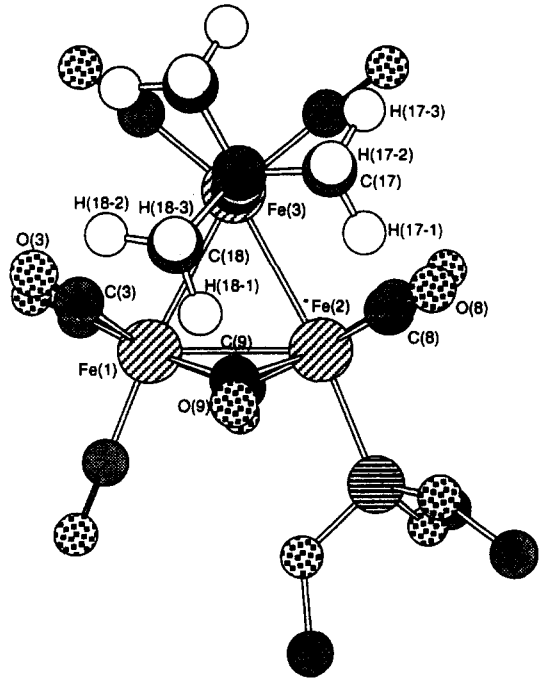

Fig. 6. The X-ray structure of one isomer of $[Fe_3(CO)_{10}(CNBu^t)\{P(OMe)_3\}]$, viewed so that the iron triangle is in the plane.

Scheme 5, as C(6)O at δ 245.7, C(11)O and C(12)O at δ 229.6, C(8)O and C(9)O at δ 215.8, $J(^{31}P^{13}C)$ = 16 Hz, C(1)O and C(2)O at δ 213.7, $J(^{31}P^{13}C)$ = 5 Hz (poorly resolved), C(3)O and C(4)O at δ 208.4, and C(5)O at δ 201.8.

CONCLUSIONS

The dynamic ^{13}C NMR spectra of $[Fe_3(CO)_{11}(CNBu^t)]$ and $[Fe_3(CO)_{10}(CNBu^t)\{P(OMe)_3\}]$ are satisfactorilyexplained using the mechanisms which have been derived for $[Fe_3(CO)_{12-n}\{P(OMe)_3\}_n]$, n = 1–3,[11] There is a low energy concerted bridge-opening bridge-closing mechanism which is still fast on the NMR timescale at even −100°C. There is also the merry-go-round mechanism which has an activation energy for 10 to 10.5 kcal mol^{-1} for $[Fe_3(CO)_{11}(CNBu^t)]$ and $[Fe_3(CO)_{10}(CNBu^t)\{P(OMe)_3\}]$. This is slightly higher than is observed for $[Fe_3(CO)_{12-n}\{P(OMe)_3\}_n]$, n = 1–3.[11] Examination of the crystal structures of $[Fe_3(CO)_{11}(CNBu^t)]$ and $[Fe_3(CO)_{10}(CNBu^t)\{P(OMe)_3\}]$ show that bridge opening is probably impeded by the large Bu^t group (see Fig. 6). In the merry-go-round, C(8)O(8) or C(3)O(3) have to move to an axial position on Fe(3). This will result in close approach to one or more hydrogen atoms on the methyl group, C(18).

EXPERIMENTAL

The NMR spectra were measured on a Bruker WH400 spectrometer. The temperatures were measured using a Comark electronic thermometer, by replacing the sample with an NMR tube containing a thermocouple in CH_2Cl_2. Carbon-13 chemical shifts were referenced to the central resonance of CD_2Cl_2 at δ 53.6. Phosphorus-31 chemical shifts were referenced to external 85% H_3PO_4, *via* the ^2H lock signal. No susceptibility corrections were made.

The following experimental procedure was used to carry out the DANTE[25] magnetization transfer measurements. A suitable temperature was chosen so that there was a little line broadening due to exchange. After the spectrometer had stabilized at that temperature, the probe was retuned, the T_1 values of the ^{13}CO groups were estimated using the $10D_1$-π-D_1-$(\pi/2)$ pulse sequence, adjusting the delay, D_1, for null signal. Subsequently, the relaxation delay was taken as $10D_1$. The DANTE pulse length was optimized for maximum signal inversion. The measurement was carried out using the pulse sequence $\{$[read FID-$\{10D_1$-$(D_2$-P_1-$(\pi/2)$-acquire$\}_8$-write FID-change $D_3]_m$-reset $D_3\}_n$, with m = 8, and n chosen to give adequate signal: noise. D_1 = 1.5 s, D_2 = 0.2 ms, P_1 = 1.2 μs, and D_3 taking values 3 μs, 0.01 s, 0.02 s, 0.04 s, 0.08 s, 0.16 s, 0.32 s and 1.5 s. T_1 (average value) was determined as 0.24 s.

The compounds $[Fe_3(CO)_{12}]$[26] and $[Fe^3(CO)_{11}\{P(OMe)_3\}]$[27] were prepared according to literature methods.

Preparation of $[Fe_3(CO)_{10}\{P(OCH_3)_3\}(CNBu^t)]$

$[Fe_3(CO)_{11}\{P(OCH_3)_3\}]$ (2.0 g, 3.33 mmol) was dissolved in toluene (200 cm^3, degassed) and heated to approximately 50°C under nitrogen. Then a solution of $CNC(CH_3)_3$ (0.28 g, 0.38 cm^3, 3.33 mmol) in toluene (20 cm^3, degassed) was added dropwise over a period of 2 h. This solution was then kept at this temperature for another 2 h while the reaction continued. The solvent was removed using a rotary evaporator and then the flask was flushed with nitrogen and placed in a freezer overnight.

The five species were separated on a silica column and three of these species were characterized using petroleum ether (b.p. range 40–65°C)–toluene (1:) as eluant. The first and last layers to be eluted off the column were obtained in very small quantities and were not characterized. The second layer consisted of $[Fe_3(CO)_4\{P(OMe)_3\}]$, the third of $[Fe_3(CO)_{11}\{P(OMe)_3\}]$, the fourth of $[Fe_3(CO)_{10}\{P(OMe)_3\}(CNBu^t)]$ and a small fifth, uncharacterized, layer. $[Fe_3(CO)_{11}\{P(OMe)_3\}]$ and $[Fe_3(CO)_{10}\{P(OMe)_3\}(CNBu^t)]$ ran very close together, and it was difficult to obtain a clean separation. The $[Fe_3(CO)_{10}\{P(OMe)_3\}(CNBu^t)]$ was always contaminated with a small amount of $[Fe_3(CO)_{11}\{P(OMe)_3\}]$. Recrystallization from petroleum ether (b.p. range 40–65°C) gave the product, 0.523 g (24%), as very dark green needles, m.p. 88°C. Mass spectrum: m/z 655 (M^+). IR (cm^{-1}) (CH_2Cl_2): 2171 [ν(C≡N)], 2061, 2018, 1996(sh), 1823.3, and 1783.4 [ν(C≡N)]. ^1H NMR (RT, CD_2Cl_2): 3.71 [$J(^{31}P^1H)$ = 13 Hz, OMe], 1.60 (Bu^t). ^{13}C (30°C, CD_2Cl_2): 220.7 (broad, CO averaged), 156.2 (very broad, CN), 53.3 (OMe), 59.5 (CMe_3), 30.1 [$C(CH_3)_3$]. ^{31}P (RT, $CDCl_2$): 161.9. Found: C, 33.1; H, 2.6; N, 2.3. $CH_{18}Fe_3NO_{13}P$ requires: C, 33.0; H, 2.8; N, 2.1%.

Crystallography

Crystal data for $C_{18}H_{18}Fe_3NO_{13}P$: M = 654.85, crystallizes from petroleum ether (b.p. range 40–65°C) as black oblongs: crystal dimensions 0.66 × 0.44 × 0.25 mm. Monoclinic, a = 11.514(3), b = 28.991(7), c = 16.498(5) Å, β = 100.13(3)°, U = 5421(3) Å^3, Z = 8, D_c = 1.605 g cm^{-3}, space group $P2_1/n$ (a non-standard setting of $P2_1/cC_{2h}^5$

No. 14), Mo-K_α radiation ($\bar{\lambda} = 0.71073$ Å), μ(Mo-K_α) = 1.803 mm^{-1}, $F(000) = 2640$.

Three-dimensional, room temperature X-ray data were collected in the range $3.5 < 2\theta < 45°$ on a Siemens P4 diffractometer by the omega scan method. The 4418 independent reflections (of 7090 measured) for which $|F|/\sigma(|F) > 4.0$ were corredted for Lorentz and polarization effects, but not for absorption. The structure was solved by direct methods and refined by full matrix least squares on F^2. Hydrogen atoms were included in calculated positions and refined in riding mode. Refinement converged at a final $R = 0.0566$ ($R_{w2} = 0.1254$, for all 7086 data, 649 parameters, mean and maximum σ/δ 0.000, 0.080), with allowance for the thermal anisotropy of all non-hydrogen atoms. Minimum and maximum final electron density −0.360 and 0.508 e Å^{-3}. A weighting scheme $w = 1/[\sigma^2(F_0^2) + (0.0653P)^2 + 6.589P]$, where $P = (F_0^2 + 2F_{c2})/3$ was used in the latter stages of refinement. Complex scattering factors were taken from the program package SHELXL93,[28] as implemented on the Viglen 486dx computer.

Supplementary material

Anisotropic thermal vibrational parameters with e.s.d.s., hydrogen atom position parameters, observed structure amplitudes and calculated structure factors.

REFERENCES

1. J. Dewar and H. O. Jones, *Proc. R. Soc. Lond., Ser. A* 1906, **79**, 66.
2. C. H. Wei and L. F. Dahl, *J. Am. Chem. Soc.* 1969, **91**, 1351.
3. (a) F. A. Cotton and J. M. Troup, *J. Am. Chem. Soc.* 1974, **95**, 4155; (b) D. Braga, L. Farrugia, F. Grepioni and B. F. G. Johnson, *J. Organomet. Chem.* 1944, **464**, C39; (c) D. Braga, F. Grepioni, L. J. Farrugia and B. F. G. Johnson, *J. Chem. Soc., Dalton Trans.* 1994, 2911.
4. (a) R. K. Sheline, *J. Am. Chem. Soc.* 1951, **73**, 1615; (b) J. W. Cable and R. K. Sheline, *Chem. Rev.* 1956, **56**, 1; (c) F. A. Cotton and G. Wilkinson, *J. Am. Chem. Soc.*, 1957, **79**, 752; (d) K. Noack, *Helv. Chim. Acta* 1962, **4**, 1847; (e) G. R. Dobson and R. K. Sheline, *Inorg. Chem.* 1963, **2**, 1313.
5. H. Dorn, B. E. Hanson and E. Motell, *Inorg. Chim. Acta* 1981, **54**, L71.
6. B. E. Hanson, C. Lisic, J. T. Petty and G. A. Iannaconne, *Inorg. Chem.* 1986, **25**, 4062.
7. M. Poliakoff and J. J. Turner, *Chem. Commun.* 1970, 1008.
8. S. Dobbs, S. Nunziante-Cesaro and M. Maltese, *Inorg. Chim. Acta* 1986, **113**, 167.
9. N. Binsted, J. Evans, G. N. Graves and R. J. Price, *J. Chem. Soc., Chem. Commun.* 1987, 1330.
10. F. A. Cotton and D. L. Hunter, *Inorg. Chim. Acta* 1974, **11**, L9.
11. See Table 13, p. 119, in B. E. Mann, *Comprehensive Organometallic Chemistry* (Edited by G. Wilkinson, F. G. A. Stone and E. W. Abe), Vol. 3, Ch. 20. Pergamon, Oxford (1982).
12. G. E. Hawkes, K. D. Sales, S. Aime, R. Gobetto and L. Y. Lian, *Inorg. Chem.* 1991, **30**, 1489.
13. S. Aime and R. Gobetto, *J. Cluster Sci.* 1993, **4**, 1.
14. R. E. Benfirled, P. D. Gavens, B. F. G. Johnson, M. J. Mays, S. Aime, J. Milone and D. Osella, *J. Chem. Soc., Dalton Trans.* 1981, 1535.
15. H. Adams, N. A. Bailey, G. W. Bentley and B. E. Mann, *J. Chem. Soc., Dalton Trans.* 1989, 1831.
16. B. F. G. Johnson and Y. V. Roberts, *J. Chem. Soc., Dalton Trans.* 1993, 2945.
17. D. H. Farrar and J. A. Lunniss, *J. Chem. Soc., Dalton Trans.* 1987, 1249.
18. M. I. Bruce, T. W. Hambley and B. K. Nicholson, *J. Chem. Soc., Dalton Trans.* 1983, 2385.
19. D. Lentz and R. Marschall, *Organometallics* 1991, **10**, 1487.
20. B. E. Mann, *Organometallics* 1992, **11**, 481.
21. B. F. G. Johnson, E. Parisini and Y. V. Roberts, *Organometallics* 1993, **12**, 233.
22. J. B. Murray, B. K. Nicholson and A. J. Whitton, *J. Organomet. Chem.* 1990, **385**, 91.
23. M. Grassi, B. E. Mann, B. T. Pickup and C. M. Spencer, *J. Magn. Reson.* 1986, **69**, 92.
24. G. A. Morris and R. Freeman, *J. Magn. Reson.* 1978, **29**, 433.
25. W. McFarlane and G. Wilkinson, *Inorg. Synth.* 1966, **8**, 181.
26. W. S. McDonald, J. R. Moss, G. Raper, B. L. Shaw, R. Greatrex and N. N. Greenwood, *Chem. Commun.* 1969, 1295.
27. G. M. Sheldrick, SHELXL93, An Integrated System for Solving and Refining Crystal Structures From Diffraction Data (Revision 5.1), University of Gottingen, Germany (1993).